HHS Public Access

Author manuscript

J Mol Biol. Author manuscript; available in PMC 2016 July 31.

Published in final edited form as:

J Mol Biol. 2015 July 31; 427(15): 2532–2547. doi:10.1016/j.jmb.2015.06.004.

Engineering synthetic antibody inhibitors specific for LD2 or LD4 motifs of paxillin

Malgorzata Nocula-Lugowska[1], **Mateusz Lugowski**[1], **Ravi Salgia**[2], and **Anthony A. Kossiakoff**[1,*]

[1]Department of Biochemistry and Molecular Biology, The University of Chicago, Chicago, USA

[2]Department of Medicine, The University of Chicago, Chicago, USA

Abstract

Focal adhesion protein paxillin links integrin and growth factor signaling to actin cytoskeleton. Most of paxillin signaling activity is regulated *via* leucine-rich LD motifs (LD1-LD5) located at the N-terminus. Here, we demonstrate a method to engineer highly selective synthetic antibodies (sABs) against LD2 and LD4 which are binding sites for focal adhesion kinase (FAK) and other proteins. Phage display selections against peptides were used to generate sABs recognizing each LD motif. In the obtained X-ray crystal structures of the LD-sAB complexes the LD motifs are helical and bind sABs through a hydrophobic side, similarly as in the structures with natural paxillin partners. The sABs are capable of pulling down endogenous paxillin in complex with FAK and can visualize paxillin in focal adhesions in cells. They were also used as selective inhibitors to effectively compete with focal adhesion targeting domain of FAK for the binding to LD2 and LD4. The sABs are tools for investigation of paxillin LD binding “platforms” and are capable of inhibiting paxillin interactions; and thereby useful as potential therapeutics in the future.

Graphical abstract

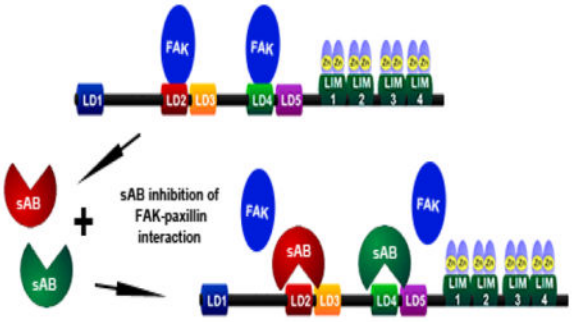

*Corresponding author: Tel: +1 773 702 9257, Fax: +1 773 702 0439, koss@bsd.uchicago.edu.

ACCESSION NUMBERS

Coordinates and structure factors have been deposited in the PDB with accession numbers 4XGZ and 4XH2.

Keywords

synthetic antigen binder; phage display; paxillin; focal adhesion; protein-protein interaction

INTRODUCTION

Adaptor proteins are a ubiquitous class of important protein molecules that function to localize and organize large multiprotein complexes at functional *loci*. They are often referred to as scaffold proteins since they generally have no intrinsic activity themselves, but rather provide the structural framework to mediate binding interactions that drive formation of large protein complexes. Their structures typically contain multiple binding modules linked together in a “beads on a string” fashion. One or several motifs are for attaching the scaffold protein at a particular site, the other motifs function to recruit and organize other binding partners around that site. In a majority of cases the scaffold proteins have motifs that are related in sequence and structure, which leads to varying degrees of specificity and cross-reactivity among the binding partners. The contrasting levels of specificity appear in some cases to be exploited by the systems to enable combinatorial production of a wide variety of different complexes.

Among the most highly studied adaptor scaffold proteins is paxillin, which acts as an essential player in forming focal adhesions. Focal adhesions serve as sites of integration of growth factor signaling and integrin pathways [1–4]. Many biological processes, such as cell motility, shape and proliferation, transcriptional regulation and mitosis have been shown to be dependent upon focal adhesion dynamics [1,5]. In its role in focal adhesions, paxillin serves as an anchor for a number of different structural and signaling proteins [1,6]. Thus, it is a nucleation site for synchronized binding of proteins that are needed to form macromolecular complexes engaged in particular signaling cascades as diverse as changes in gene expression and reorganization of the cytoskeleton [7,8]. Because paxillin is one of central proteins within the focal adhesion, it is also a common target of many different oncoproteins such as BCR/ABL, v-Src and E6 [8] and is also overexpressed in a number of different cancers, including renal and lung carcinomas as well as breast tumors [9]. Typical of scaffold proteins, paxillin is rich in multiple protein-protein interaction motifs [10,11]. Its N-terminal section is thought to control most of its signaling activity and is comprised of five so-called LD motifs (LD1-LD5) (Fig. 1a) [1]. LD motifs provide the attachment sites for other focal adhesion proteins, such as focal adhesion kinase (FAK) [11,12], vinculin [6,13], α-parvin [14], integrin-linked kinase (ILK) [15] and also for papillomavirus E6 protein [16,17]. Additional sites of interaction in the paxillin molecule include SH2- and SH3-binding domains that mediate association with the Crk, Src and Csk families [11]. In the C-terminal part of paxillin, four LIM domains (LinII, Isl-1 and Mec-3) target paxillin and its binding partners to focal adhesions [13].

The name for the LD motifs is derived from the first two amino acids of their consensus sequence LDXLLXXL [1,13]. These motifs contain approximately 20 residues and are characterized by their leucine-rich sequences. LD domains are highly conserved in paxillin sequences from different, even very distant species like humans, chicken and even

Dictyostelium. Additionally, LD motifs are conserved between other members of the paxillin family, like Hic-5 (name derived from 'hydrogen peroxide inducible clone') or leupaxin [1]. LD motifs are multispecific, as they are generally capable of binding different partner proteins, and these partner proteins can themselves bind to more than one motif [13,18,19]. Isolated LD motifs 1, 2 and 4 have been crystallized in complex with their corresponding protein partners, and have been shown to form amphipathic helices in the bound state that interact *via* the hydrophobic side of the helix [20–23,9,24,25].

Paxillin is heavily phosphorylated, both at Tyr and at Ser residues. This has been shown to be important for regulation of focal adhesion dynamics in cell motility (reviewed extensively in [7,16]). Several kinases contribute to the phosphorylation patterns of paxillin, among those FAK and Src were the first to be found to be crucial in paxillin signaling [26]. Additionally, paxillin interacts with cell surface receptors and the actin cytoskeleton and activates several signal transduction pathways that are known to regulate normal cell physiology. FAK's interaction with paxillin motifs LD2 and LD4 occurs through its C-terminal focal adhesion targeting (FAT) domain, which directs the localization of the kinase to focal adhesions [11,12]. Once localized through paxillin attachment, FAK is further responsible for phosphorylation of a number of proteins at focal adhesions dependent on integrin-mediated signaling [27]. Because paxillin is one of central proteins within the focal adhesion, it is also a common target of many different oncoproteins and is also overexpressed in a number of different cancers.

Current attempts to establish the full spectrum of activities of the paxillin-FAK interaction have been frustrated by the lack of requisite tools and reagents that could systematically characterize the functionality of these complex associations. To overcome this barrier, we have developed a powerful set of reagents for sorting out cause and effect relationships in the paxillin-FAK system. Using novel high performance phage display libraries, exquisitely specific synthetic antibodies (sABs) to the LD2 and LD4 of paxillin, the two recognition sequences for FAK, have been generated. The sABs are based on an antibody Fab domain whose scaffold has been engineered to be highly stable and non-immunogenic. The sABs bind to their corresponding LD motifs with nM affinity, and they are completely specific to their target LD motif without detectable cross-reactivity. The structures of LD-sAB complexes demonstrate that the binding occurs in large part *via* hydrophobic side of the LD helix, overlapping and extending outside of the epitope that is utilized by natural paxillin partners. Our work demonstrates that the sABs can be used as effective tools to separately probe the binding of paxillin partners, as each of them is capable of staining paxillin in focal adhesions and of pulling down paxillin with its natural partner – FAK. Finally, the sABs can effectively compete with the FAT domain for the binding to LD2 and LD4 providing insight for how they might be utilized to intervene and deter the cell from initiating a particular behavior or to reprogram a response.

RESULTS

Phage display and selection

Composition of LD2 and LD4 peptides—Available crystal structures of LD2 and LD4 with paxillin protein partners (FAK (PDB: 1OW6, 1OW7, 1OW8 and 2L6G); Pyk2 (PDB:

3U3C); α-parvin (PDB: 2VZG and 2VZI)) reveal that in their bound state, the motifs form an amphipathic helix that extends past the LD motifs [20–22]. This finding suggested that additional amino acids outside of core LD motifs might be crucial for their specificity [20]. Therefore, four additional residues were included on both the N and C terminal ends flanking the core 8 amino acids of consensus LD motif sequence (Fig. 1b). The nomenclature adopted here for the comparisons of the LD motifs is that the first Leu residue in the consensus LD sequence is designated position 0. Residues following this position are numbered: 1 to 11. Residues N-terminal to this position are numbered in descending order: −1 to −4 (Fig. 1b).

Peptide formats and phage display selections—To generate synthetic antibodies (sABs) to the LD2 and LD4 domains, a synthetic phage display library with a diversity of 10^{10} Fab fragments was employed. Fab fragments were displayed as fusions to the minor coat protein pIII of M13 bacteriophage (Fig. 2a). In the library, diversity was introduced into four of the six complementarity determining regions (CDRs) loops (L3, H1, H2 and H3) (Fig. 2b), as described previously [28,29].

For phage display selections, the target is generally biotinylated for immobilization to streptavidin magnetic beads to facilitate the phage capture and washing steps. However, insolubility, which is a general issue with hydrophobic peptides like the LD motifs, can be exacerbated upon addition of biotin. To circumvent this problem, the LD peptides were expressed as C-terminal fusions of maltose binding protein (MBP-LD) to improve the solubility and prevent the peptides from sticking to the plastic surfaces thus, maximizing the accessibility of the epitope and minimizing background binding.

Four rounds of phage display selection were performed on both MBP-LD2 and MBP-LD4. To avoid selection for MBP binders concurrently with binders to the LD targets, a competition selection strategy was employed. In order to eliminate all the potential contaminating MBP binders the phage display library was pre-incubated with a high concentration of MBP prior to the first round of phage sorting. Additionally, an excess of free MBP has been used as a competitor in all subsequent steps of sorting (Fig. 2a). This way, all library members that bind to MBP were engaged in interactions with soluble non-immobilized protein. This effectively eliminates MBP binders from being pulled down along with the LD binders. Based on this procedure, two unique sABs were identified, one binder per each LD peptide by testing the selected clones with phage ELISA (Figs. 2b and S1).

sABs bind to LD2 and LD4 with high affinity and selectivity—The selected sABs were expressed and purified in protein format as Fab fragments and subjected to further analysis by equilibrium surface plasmon resonance (SPR) to assess their binding affinities. The K_D value for LD2 sAB was estimated to be 24 nM, and the K_D value for LD4 sAB was estimated to be 6 nM (Fig. 2c). The two sABs did not bind to isolated MBP, and importantly, did not cross react with the other LD peptide (Fig. 2c). This indicated that the sABs bound only their individual targets with high affinity and specificity.

LD-sAB structures

To establish the nature of LD-sAB binding interface, the crystal structures of LD2-sAB and LD4-sAB complexes were determined with 2.5 Å and 2.0 Å resolution, respectively. The complexes were crystallized by mixing the sABs purified in protein format with the LD motifs in the format of synthesized peptides. The crystallographic refinement statistics are presented in Table 1. A notable feature of the crystals is that they contained multiple copies of their respective complex in the crystallographic asymmetric unit (ASU). While this situation made the determination and refinement of the structures more difficult, it provided for multiple independent copies that could be compared to identify any conformational variability in the bound LD peptide structures. The ASU contained twelve (LD2) and six (LD4) independent copies of peptide-sAB complexes (Fig. S2a and b). By comparing these multiple copies of the sAB-LD complexes within each asymmetric unit, we were able to demonstrate that variation among the copies was small indicating that the structures provide an accurate picture of how the peptides bind to their respective sABs.

The sABs bind LD domains in their native helical conformation—The structures revealed that both LD peptides are in the α-helical conformation when bound to their cognate sABs (Fig. 3a, underlined sequences), and that the peptide helices are aligned along a groove formed by the four diversified sAB CDR antigen binding loops (Fig. 3; Fig. S2c and d). Interestingly, the peptides are positioned in the opposite directions with respect to the sAB CDR loops (compare Fig. 3b top and bottom panel). LD2 is docked through its N-terminal end to CDR-L3 of the light chain and the helix is surrounded by the loops from heavy chain (CDR-H1, -H2, -H3) (Fig. 3b and c top panel). In contrast, the N-terminal part of LD4 is stabilized by the heavy chain CDR-H3 and the remaining three diversified loops, CDR-H1, -H2 and -L3, frame the peptide on both sides (Fig. 3b and c bottom panel).

Specificity determinants—The two LD domains have a similar sequence signature and the sAB interfaces share some features. One common feature in both LD2- and LD4-sAB structures is that the side chain of Asp 1 of the peptide forms hydrogen bonds with hydroxyl groups of Ser 33 in CDR-H1 and tyrosine residues in CDR-H2 of the LD2-sAB (Tyr 52 in LD2 sAB and Tyr 50 in LD4 sAB) (Fig. 4, top panels). However, overall, their differences are more prevalent and these may explain the high specificity of the raised sABs for their particular LD domain. For example, there is an additional hydrogen bond formed between Thr (−3) of LD4 and Ser 33 of the sAB (Fig. 4b; top panel). This is possible because the LD4 peptide has three fewer Leu residues than LD2, as Leu residues at positions −3, 4 and 5 in LD4 are substituted by Thr, Met and Ala residues, respectively (Fig. 1b). Consequently, the interactions are more diverse in the LD4-sAB structure than those of LD2-sAB (Fig. 4). In the LD2-sAB complex, the positioning of the sAB's CDR H2 loop orients a string of five Tyr residues (Tyr 52, 53, 54, 56, 58) coincident with the Leu-rich hydrophobic face of the peptide helix. In fact, all of the Tyr residues found within the three diversified loops of the LD2 sAB heavy chain interact with all five of the Leu residues present in the LD2 peptide (Fig. 4a; bottom panel). In contrast, the LD4 sAB has only three Tyr residues in the CDR H2 loop (Tyr 50, 56, 58) and they are all grouped in the vicinity of the hydrophobic side chain of Met (−4) of the peptide (Fig. 4b; bottom panel). Here, the hydrophobic face of the peptide helix is shielded by the CDR L3, which is exceptionally long (8 residues), hydrophobic at its

base and positively charged at the top of the loop. The basic residues present in that loop appear to stabilize the flexible hydrophilic C-terminal part of the peptide. In comparison, in the LD2-sAB structure, CDR L3 interacts with the N-terminal part of the helix (Fig. 4a; top panel), through backbone-backbone hydrogen bonds. In both LD-sAB interfaces the first turn of the peptide helix is distorted and the internal hydrogen bond between residues i-(i+4) is mediated through water (Fig. 4; top panels).

sABs as biological reagents

The sABs recognize full-length native paxillin in cellular environment—To assess the ability of the anti-LD sABs to bind endogenous full-length paxillin, a set of immunoprecipitation experiments from cell lysates was performed (Fig. 5a). Pull-down experiments of paxillin using increasing concentrations of both a mixture of the two LD specific sABs and each of the sABs alone were analyzed by Western Blot. The observed band of a 68 kDa protein is consistent with the known molecular mass of the endogenous heavily phosphorylated full-length paxillin molecule [6]. Thus, even though selected against short 16-amino acid peptides, each of the sABs and a mixture of both of them are capable of recognizing and pulling down full-length paxillin found in cells. Notably, the intensities of the paxillin bands obtained after pull down with each of the sABs are lower than the signals obtained after pull down with both of the sABs. That indicates that paxillin is not saturated with the binders, and as a result, even in the presence of both of the sABs, one sABs is bound per one paxillin molecule.

The sABs pull-down paxillin-FAK complexes—As shown by the immunoprecipitation experiments, the sABs are capable of pulling down full-length paxillin in its physiological state through engaging only one LD motif. Since the non-corresponding LD motif is left free for binding it raised a question whether the sABs are able to precipitate paxillin in complex with its natural partner – FAK. In this regard, it has been determined that both sABs are capable of pulling down paxillin-FAK complex from cell lysates (Fig. 5b). Similarly to paxillin bands, the intensity of the bands corresponding to FAK seems to be approximately additive. This observation is in accordance with the fact that the concentration of the sABs is below the paxillin saturation point. Since the sAB-LD interaction is tight and specific (Fig. 2c), it seems logical that LD2 sAB pulls down FAK-paxillin complex by FAK-LD4 interaction and LD4 sAB precipitates the complex formed by FAK-LD2 binding.

sABs as immunostaining reagents—To test whether the LD sABs are specific and able to identify paxillin at focal adhesions by immunofluorescence, a series of immunostaining experiments using the A549 lung cancer cell line was performed (Fig. 5d). It is well established that focal adhesions appear as dense clearly defined microstructures at the end of actin fiber bundles [30]. Microphotographs obtained with LD sABs labeled with Cy-5, indicate that the sABs localize in focal adhesions in the expected regions of the cell (Fig. 5d; white arrows). There is no detectable level of auto-fluorescence in the red channel, as assessed from untreated control cells (Fig. 5d). The cytoplasmic fluorescence most probably comes from sABs bound to free paxillin yet to be recruited into focal adhesion complex, as it is not present in the sAB untreated cells (Fig. 5d).

Exploiting sABs as potential focal adhesion inhibitors—Binding between the FAT domain of FAK and paxillin occurs through interactions with the LD2 and LD4 motifs. Disruption of these interactions has the potential of affecting the process of focal adhesion assembly and turnover by influencing both FAK and paxillin downstream signaling. Thus, the LD2 and LD4 sABs were tested as potential competitive inhibitors of FAK-paxillin interaction. To this end, the LD2 and LD4 peptides were produced as fusions to MBP in a similar format to what was used in the phage display selections to ensure that the hydrophobic peptides remain soluble in solution. MBP-LD fusions at a concentration in the FAT-LD affinity range (5 μM; Fig. S3) were allowed to equilibrate with their corresponding sABs. Then, a three hundred fold higher concentration (1.5 mM) of purified recombinant FAT was introduced. The resulting complexes were immunoprecipitated by the sABs and detected with an antibody against 6xHis-tag present on MBP (Fig. 5c; compare the intensity of the +/− FAT lanes). Thus, a decrease in the band intensity in Fig. 5c obtained after incubation with FAT measures the competition between the sAB and FAT for binding to the LD motif. As anticipated, based on measured affinity of the FAT domain compared to the sABs for their LD motifs, even a millimolar concentration of FAT was not sufficient to outcompete either of the anti-LD sABs from their binding sites. However, small differences in the drop of the signal between the two LD motifs suggest that the anti-LD2 sAB had weaker inhibitory properties compared to the anti-LD4 sAB. This might be a result of the fact that LD2 sAB binds weaker to its corresponding peptide than the LD4 sAB. Additionally, FAT interaction with MBP-LD2 is stronger than FAT interaction with MBP-LD4 (Fig. S3). This effect might be also enhanced by the fact that there are two LD2 binding sites and only one LD4 binding site on FAT [31], so the effective LD2 binding site concentration in the experiment was twice as high as the effective LD4 binding site concentration.

DISCUSSION

A key objective of our work was to generate a set of reagents that could assist in systematically characterizing the functions of paxillin LD motifs in focal adhesion dynamics. Paxillin is an essential adaptor protein that plays a central role in recruiting and organizing partner proteins to form the requisite macromolecular complexes needed for focal adhesion function [8]. Details of how this process works at a molecular level remain sparse because of the lack of adequate tools and reagents to analyze the component steps. The protein recruitment process to nucleate and regulate focal adhesions is dependent on multiple recognition motifs in the paxillin molecule, among which peptidic LD motifs seem to be of paramount importance for signal transduction. A question of particular interest is how FAK specifically targets the paxillin LD2 and LD4 domains, either as individual domains or together. Below we discuss the challenges in obtaining the relevant data that speak to these issues and the approaches that were used to obtain them.

Generating specific sAB binders to LD2 and LD4

To help address the role of the LD domains in binding to FAK, we used phage display to generate synthetic antibodies (sABs) that were selected to potentially interfere with binding to either LD2 or LD4. In designing the most representative LD peptides to be used in the

phage display selections, we relied on two pieces of structural information. First, LD domains have a helical structure when bound to their targets and second, binding and specificity involve not only their eight amino acid LD motif, but also several flanking residues extending off either side [20–22]. These eight residues, four on each end of the core motif, serve as important specificity determinants as well as for increasing the helical propensity of the peptide. The chosen peptides consisted of 16 amino acids.

Phage display selections to generate high affinity and specific sABs against short peptides are generally more challenging than for larger proteins. In many cases, a poorer diversity of binders is obtained for peptide targets, even at lower selection pressure. Additionally, anti-peptide antibodies are typically of lower affinity than anti-protein antibodies [32]. In the case of the LD peptides, to enable successful selections, we had to overcome two technical challenges. The first derives from basic thermodynamics. Free peptides are inherently flexible and their binding to any protein comes at a significant entropic cost [33]. Importantly, in the case of the LD peptides, the entropic penalty is somewhat abated because they have the natural propensity to form α-helical structures in their bound state [18–22,24,25,34]. Thus, we supposed by including the additional flanking regions mentioned above, we would not be targeting a random coil peptide, but a reasonably structured entity. The fact that the peptides bind to the resulting sABs at very high affinities and as helices indicates this assumption was correct.

The second challenge we had to address was the solubility issue. The eight amino acid LD motifs are extremely hydrophobic, even in the context of the extended peptides. Even though the flanking residues are less hydrophobic than the LD motifs themselves, we found the peptides tended to aggregate under conditions normally used for phage display selections. To overcome this, we fused the LD2 and LD4 peptides onto the C-terminus of maltose binding protein (MBP-LD). MBP fusions of this type have been shown to be effective solubilization chaperones for poorly soluble targets in phage selections. It is noteworthy however, that there are some tradeoffs in using this strategy. MBP is a highly antigenic protein itself and a vast majority of binders that are selected in each step would target MBP, not the peptide if not corrected for. Therefore, a series of steps were taken to prevent the MBP binders from being pulled-down and amplified during the phage display selections. The phage display library was saturated with free MBP prior to selection and a high concentration of free MBP was added during all steps of the selections to “soak up” all the MBP binding phages. Additionally, rigorous washing steps were required to ensure no MBP binders were carried through and contaminate the final pool of peptide binders making it unavoidable that in the process, some of the peptide binders are also washed off and lost to the pool.

Taken together, these highly stringent competition and clearing steps resulted in producing a very limited number of sABs for each LD domain. In fact, we determined that only one sAB for each domain displayed the desired characteristics we sought for use as high performance biological reagents. However, for the applications used here, a single high affinity and specific sAB is sufficient. We note that lowering the selection stringency might recapture some of the lower affinity and specificity binders that still could be useful, but this comes at the cost of contaminating the pool with these clones, making it an unattractive option. Thus,

in hindsight, the ultra-high stringency of the phage display selections was necessary to isolate the rare examples of sABs that display both such high affinity and specificity considering the nature of the input LD targets.

The conformation of the LD motifs in complex with the sABs and FAT domain of FAK

Structural studies have shown that the FAT domain binds the helical forms of the LD2 and LD4 motifs [20]. A comparison of the FAT-LD structures with the structures of LD motifs bound to their corresponding sABs indicate a number of similarities (Fig. 6a and b) [20]. The structural alignment of the Cα atoms of 10-amino acid helical fragments of LD2 ($_{-1}$ELDRLLLELN$_{8}$) and LD4 ($_{-2}$RELDELMASL$_{7}$) in the structures with sABs and FAT gives root-mean-square deviation (RMSD) values of 0.52 Å and 0.60 Å, respectively. In the LD2-sAB structure, the first 2 amino acids of the peptide helix are oriented such that the first turn of the helix is distorted. Thus, the RMSD between the Cα atoms of a longer 12-amino acid fragment of LD2 ($_{-3}$LSELDRLLLELN$_{8}$) bound to the sAB and FAT is higher −0.93 Å. A similar situation occurs in the case of the first amino acid of the LD4 helix (T(−3)). The RMSD between the Cα atoms of this 11-residue fragment ($_{-3}$TRELDELMASL$_{7}$) is 0.73 Å. The fact that the peptides bind to the sABs in a similar conformation as observed when bound to their natural protein partner suggests that the sABs should be capable of recognizing LD motifs in the full-length paxillin in the cellular environment. Accordingly, each of the sABs proved to be able to recognize its corresponding LD motif in full-length paxillin both in cell lysates (Fig. 5a) and in the context of focal adhesion environment (Fig. 5d).

Comparison of how the LD domains bind the sABs and FAT domain of FAK

The LD peptides produce more extensive contacts with the sABs than with the FAT domain. This is because the CDR binding loops of the sABs form deep binding clefts. Thus, while the overall buried surface area in LD2-FAT structure is less than ~480 Å^2, in LD2-sAB the burial is substantially larger: ~690 Å^2 (Fig. 7a). Even larger differences are observed in the case of LD4 peptide. The overall buried surface area in LD4-FAT interface is ~420 Å^2, whereas in LD4-sAB it is ~750 Å^2 (Fig. 7b).

It has been proposed based on FAT-LD2 and FAT-LD4 structures that the key contacts between LD motifs and FAT are made by hydrophobic residues at positions −3, 0, 3, 4 and 7 of the LD peptide and an ion-pairing between two Lys residues of FAT and two acidic residues present in both LD2 and LD4 (Glu-1, and Asp 1) that define the directional orientation of the peptides [20]. Interestingly, the sABs utilize the same hydrophobic side of the LD domains' amphipathic helix as the FAT domain, but in different ways. In the LD2-sAB structure the peptide is rotated in the sAB binding pocket such that it binds the same hydrophobic side of the LD helix as FAT, but additionally grasps the peptide on the other side where it not only makes contacts, but substantially buries side chains of Ser(−2), Asp 1 and Leu 5 (Fig. 7a and top panel of Fig. 3a). On the other hand, LD4 utilizes exactly the same side of the helix for interactions with FAT and the sAB, but it is so extensively buried within the sAB binding pocket that there are only two residues that do not take part in the sAB binding (Arg (−2) and S2) (Fig. 7b and bottom panel of Fig. 3a).

Application of the anti-LD2 and LD4 sABs as biological reagents

It was previously shown that although a single functional LD motif (LD2 or LD4) is sufficient for proper localization of FAK to focal adhesions, a simultaneous binding to both of the recognition motifs is required for FAK to reach its full activation and downstream signaling [31]. The binding affinity of the FAT domain to individual LD motifs is relatively weak. Our results reveal a μM affinity between human recombinant FAT domain and the individual LD motifs fused to MBP (Fig. S3). Additionally, longer fragments of avian paxillin containing either LD2 or LD4 and fused to gluthathiono-S-transferase (GST) were shown to bind to FAT with comparable affinity of around 4 μM, which, even with its avidity effect due to its dimerization through the GST fusion, is ten times weaker than the affinity displayed by the paxillin fragment containing both LD2 and LD4 [35]. In contrast, however, the sABs bind to their corresponding LD motifs with nM affinities.

Because of the relatively weak interaction between the FAT domain and the individual LD motifs, we sought to determine whether we could exploit the high affinity of the sABs to effectively compete with the FAT-LD interactions. Indeed, we determined that a very high concentration of the FAT domain is required for it to compete with the sABs for the binding to the LD motifs. Thus, we could postulate that in the cell, when a physiological concentration of FAK and paxillin is present, the sABs would bind to LD2 and LD4 and readily displace FAK from endogenous paxillin molecule. However, it has been shown by the paxillin pull down experiments that, in the sAB concentration range that is below paxillin saturation point, the sAB-paxillin complex is preferentially formed in 1:1 ratio even when both of the sABs are present in the cell lysate. This allows for the sABs to be used as immunoprecipitation reagents capable of pulling down paxillin partner - FAK - along with paxillin *via* the second LD motif. This experiment demonstrates that FAK is able to bind to paxillin through LD2 or LD4 independently and still form a complex that is stable enough to be precipitated through either the LD2- or LD4-sAB interaction. This result suggests that the dissociation of the FAK – paxillin complex could not be achieved by inhibition of the binding of only one of the two LD motifs to the FAT domain, as it was elegantly proposed by Bertolucci and others [34].

Another advantage of the sABs' high specificity and affinity to their corresponding LD motifs is that the fluorescently labeled sABs can be used as primary immunostaining reagents detecting endogenous paxillin molecules in fixed cells without requiring the use of secondary IgG conjugates or reporters for signal enhancement. This feature allowed us to observe that the sABs stain paxillin in focal adhesions in a notably different manner. Specifically, the LD2 sAB tends to detect twice as much of the large focal adhesions (3–15 μm^2) than the LD4 sAB (Fig. S4). What is more, the LD2 sAB is also able to detect the largest (> 6 μm^2) focal adhesions that the LD4 sAB does not recognize. This could be a result of a physiological state of paxillin in large focal adhesions that can be discerned by our tools. This suggests that the sABs could be readily utilized as reagents to probe LD2 or LD4 function separately. As paxillin has been shown to be important in various disease states as well as cancer, it would now be useful to determine the efficacy of these sABs in those models.

MATERIALS AND METHODS

Protein expression and purification

Peptides corresponding to LD2 and LD4 of human paxillin, spanning amino acids 141–165 for LD2 and 262–277 for LD4 were fused to MBP at the C-terminus. Primers coding for peptides had all rare codons substituted with codons optimal for *Escherichia coli*. Primers were annealed with each other in order to form a double stranded DNA constructs and then they were annealed with pMCSG9 vector at the ligation independent cloning (LIC) site. The vector contains sequences coding for a 6xHis-tag and a TEV protease site followed by MBP. The LIC site is at the 3′ terminus of MBP cDNA.

Fusion proteins were expressed in BL21(DE3) cells grown at 37°C in 2xYT media supplemented with 100 μg/mL ampicillin until OD_{600} reached 0.5–0.7. After the OD_{600} was reached, 1 mM IPTG was added and the cultures were grown in 30°C overnight. The cells were harvested, re-suspended in Ni-NTA loading buffer (50 mM Na_2HPO_4, 300 mM NaCl, pH 7.5) and lysed using French press. After 1 h centrifugation, the supernatant was loaded onto HisTrap 5 mL column (GE Healthcare), and the proteins were eluted with a linear gradient of 0–250 mM imidazole. Fractions containing proteins were pooled, diluted 10 times with IEX buffer (10 mM TRIS, pH 7.5) and loaded onto HiTrap Q 50 mL column (GE Healthcare). The recombinant proteins were eluted with 50 mM to 2 M NaCl gradient. Fractions containing pure MBP-LD fusions were pooled and frozen at −80°C. Isolated MBP was expressed and purified from the empty pMCSG9 vector according to the procedure described above.

Phage display selection

For phage display selections MBP-LD2 and MBP-LD4 were chemically biotinylated with NHS-SS-PEG4-Biotin reagent (Thermo Scientific). The reagent allows for mild elution from streptavidin-coated surfaces with the use of reducing agents. Proteins at 100 μM concentration were mixed with a 10-fold molar excess of biotinylation reagent in the reaction buffer (50 mM Na_2HPO_4, pH 7.5, 100 mM NaCl). The reaction was performed at room temperature (RT) for 60 min and was quenched by addition of 1/10 v/v of 1 M TRIS pH 7.5. Biotinylation was verified by mass spectrometry and a pull-down assay using Streptavidin MagneSphere® Paramagnetic Particles (PMPs, Promega).

Phage display selection was performed as follows. 1 ml of phage library containing ~10^{12}–10^{13} colony-forming units (cfu) of phages was combined with TBS buffer containing 4% PEG 8000 and 0.5 M NaCl and precipitated for 1 h on ice. The pellet of precipitated phages was re-suspended in 0.5 mL of 80 μM solution of free MBP in TBST-BSA buffer (TBS supplemented with 0.1% (w/v) Tween 20 and 0.5% (v/v) BSA) and incubated for 15 min on ice. PMPs, prewashed three times with the same buffer, were incubated with 100 nM of biotinylated MBP-LD2 or MBP-LD4 for 15 min at RT. The solution containing unbound fraction was discarded and PMPs with bound proteins were re-suspended in TBST-BSA containing 5 μM biotin to block unoccupied streptavidin and limit non-specific binding. After 5 min incubation at room temperature, PMPs were washed three times with TBST-BSA. After washing, PMPs with different bound proteins were combined, pulled down and

the supernatant was discarded. Combined PMPs were re-suspended in the phage-MBP solution. After 1 h incubation with mixing, the supernatant containing unbound phages was discarded and PMPs were gently washed twice with fresh portion of TBST-BSA containing free MBP. Pulled down PMPs with bound phages were used to infect *E. coli* XL1-Blue cells (Stratagene) for overnight phage amplification at 37°C. The amplified phages were submitted to additional three rounds of biopanning, in which phage solution in TBST-BSA containing MBP was incubated separately with free MBP-LD2 or MBP-LD4. All subsequent rounds of selection were performed at RT using KingFisher magnetic particle processor (Thermo Scientific). The instrument automatically performed binding of protein-phage complexes to PMPs, blocking with biotin, four steps of washing in TBST-BSA-MBP buffer and elution of complexes with 100 mM DTT in 20 mM Tris, pH 8.0. For phage amplification in each round of phage sorting, the phages after elution were used to infect XL1-Blue cells that were in logarithmic phase. In the second round of selection binding of phages was performed in presence of 50 nM protein and 5 μM of free MBP. In the subsequent rounds the concentration of proteins was decreased to 10 nM, and the concentration of free MBP was decreased to 1 μM. Thus, in every round of selection, free MBP was kept at a 100 × molar excess over the MBP-LD fusion.

Phage ELISA

A single-point competitive phage ELISA was performed to select the clones that bind to MBP-LD2 and MBP-LD4 and not to free MBP. Individual clones from the fourth round of selection were grown in a 96-well format in 400 μL of 2xYT media supplemented with ampicillin and M13-KO7 helper phage (New England Biolabs). Culture supernatants were diluted five times in PBST-BSA buffer (PBS with 0.5% (w/v) BSA and 0.1% (v/v) Tween 20) and incubated for 15 min at RT with free MBP or MBP-peptide fusions. Then, the solution was transferred to neutravidin coated plates with immobilized biotinylated MBP-LD2 or MBP-LD4 (50 μL of 20 nM solution). Plates were incubated for 15 min at RT and then washed three times. After washing, horseradish peroxidase conjugated with an anti-M13 antibody (1:5000 dilution in PBST-BSA buffer) was added and was allowed to react with bound phage for 30 min. The plates were washed again and were developed with 3,3′, 5,5′-tetramethyl-benzidine and H_2O_2 peroxidase substrate (Thermo Scientific) until yellow color appeared. The reaction was quenched with 1 M H_3PO_4 and absorption at 450 nm was determined. The ratio of A_{450} in the absence and in the presence of competitor (free non-biotinylated protein) was calculated and clones that had the strongest signal and the best competition ratio were submitted for sequencing.

Surface plasmon resonance

The binding affinity of the sABs to the MBP-LD fusions was determined *via* equilibrium SPR on a Biacore 3000 instrument. Approximately 70 response units (RU) of each of the 6xHis-tagged MBP-LD proteins (50 nM) were bound to the surface of the Ni-NTA sensor chip (GE Healthcare) through the N-terminal His-tag. Purified sABs at concentrations ranging from 1 nM to 1 μM, were injected onto the chip surface until the equilibrium of the binding was reached (the sensogram was stable). Similarly, the binding affinity of FAT domain of FAK to MBP-LD proteins was determined with equilibrium SPR.

In that case the MBP-LD proteins were bound to Ni-NTA sensor chip surface at a concentration of 100 nM. FAT was injected in the concentration range of 0.02–10 μM until the equilibrium was reached. In all cases, the binding responses were double referenced by subtraction of responses when the buffer was flowed over the bound target, and by subtraction of the signal obtained after flowing the sAB in the blank cell (the cell with no target protein immobilized). Data were processed using Scrubber (BioLogic Software, Campbell, Australia). For the binding curves, the signal from the stabilized equilibrium part of the sensogram was plotted against the concentration of the sAB.

sAB expression and purification

The phage representing two clones that exhibited binding in the phage ELISA experiments were used to infect XL-1 Blue cells. The phagemid DNA was purified and used as a template for QuickChange mutagenesis that introduced a STOP codon between the sequences coding for the heavy chain of the sAB and pIII phage coat protein. Phagemid with a STOP codon was then transformed into *E. coli* 55244 expression cells. The cells were transferred to 15 mL of 2xYT media supplemented with 100 μg/mL ampicillin and 10 μg/mL kanamycin and grown overnight at 37°C. 10 mL of the culture was used to inoculate 1 L of 2xYT supplemented only with ampicillin. After ~20 h incubation at 30°C with shaking, the cultures were spun down and the pellet was re-suspended in 1 L of phosphate depleted CRAP-Pi media containing 100 μg/mL ampicillin (27 mM $(NH_4)_2SO_4$, 14 mM KCl, 2.4 mM sodium citrate 5.4 g/l yeast extract, 5.4 g/l HyCase SF Casein, 0.11 M MOPS buffer, pH 7.3, 0.55% (w/v) glucose and 7 mM $MgSO_4$). CRAP-Pi media allow for efficient expression from plasmids containing *phoA* promoter. The cultures were grown overnight at 30°C. Cell pellets were re-suspended in 20 mM Na_2HPO_4 pH 7.5, 500 mM NaCl supplemented with DNase I (20 μg/mL), hen egg lysozyme (100 μg/mL) and protease inhibitors (1 mM PMSF, 2.5 μg/mL leupeptin, 1 μg/ml aprotinin and pepstatin) and lysed using French press homogenizer. The lysates were incubated at 65°C for 30 min to get rid of a majority of impurities and centrifuged at 30000 × *g*. The supernatant was loaded onto HiTrap rProtein A Fast Flow column (GE Healthcare) in the lysis buffer and the sAB was eluted with step gradient of 0.1 M acetic acid. The whole elution from the column was then loaded onto Resource S column (GE Healthcare) equilibrated with sodium acetate pH 5.0. Pure sAB was eluted from the column with a linear gradient of NaCl. The fractions containing the sAB were combined, concentrated and dialyzed overnight to a buffer appropriate for subsequent experiments. Due to the way the library was constructed, all sABs are rich in hydrophobic residues, mostly Tyr, and tend to elute from Superdex columns later than what is expected from their molecular weight. When size exclusion is performed with the sABs bound to the corresponding LD peptides or MBP-LD constructs the complexes elute according to their molecular weight (data not shown). This strongly suggests that sABs are not forming aggregates but are retained by the column's resin itself.

Crystallization

LD2 sAB in 10 mM HEPES pH 7.5, 100 mM NaCl was concentrated to 14 mg/mL and mixed with 3 molar equivalents of LD2 peptide (Anaspec; NLSELDRLLLELNAVQHNPP), such that the final protein concentration was 10 mg/mL. The proteins were incubated for 0.5 h on ice, and spun down at 21000 × *g* for 10 min. Crystallization was performed by the

hanging drop vapor diffusion method, by mixing one volume of the complex with one volume of the reservoir (20% PEG 3350, 0.2 M $NaNO_3$). The drop was equilibrated against 0.5 mL of the reservoir. Crystals of LD4 sAB with the peptide were obtained by concentrating the sAB in 10 mM HEPES pH 7.5, 100 mM NaCl to 56 mg/mL and mixing with 3 molar equivalents of LD4 peptide (Peptide 2.0; WGGSATRELDELAMSLSDFK), such that the final protein concentration was 32 mg/mL. After incubation for 0.5 h on ice, and spinning down at 21000 × *g* for 10 min, crystallization was also performed using the hanging drop vapor diffusion method, by mixing one volume of the complex with one volume of the reservoir (18% PEG 8000, 0.1 M MES pH 6.5, 0.5 % n-Dodecyl-N, N-Dimethylamine-N-Oxide (LDAO)). The drop was equilibrated against 1 mL of the reservoir.

Data collection and processing

For data collection, the crystals were harvested using CryoLoops (Hampton Research) and mixed with the cryo-protecting solution containing the same components as the reservoir with addion of 20% ethylene glycol (LD2) or glycerol (LD4). Then, the crystals were harvested again and flash-frozen in liquid nitrogen. Data were collected at Advanced Photon Source at beamline 24-ID-C with Pilatus 6 M detector. The data were indexed, integrated and scaled with either HKL-3000 (LD2) [36] or XDS (LD4) [37] and the phases were obtained by molecular replacement using Phaser [38] with anti-MBP sAB from MBP-sAB structure (PDBID: 3PGF) as a searching model). The models were rebuilt with Buccaneer (CCP4 suite) [39] and refined using Refmac [40] and Coot [41]. Figures were created with PyMol [42].

Cell culture

A549 cells (ATCC) were grown in DMEM (Cellgro) supplemented with 1% Pen Strep (Gibco) and 10% FBS (HyClone). For immunostaining experiments, approximately 1×10^5cells were grown in 12 well plates on 18 mm circular glass slides. For immunoprecipitation experiments, cells were grown in T75 flasks to monolayer, then detached with 0.05% Trypsin/EDTA (HyClone), washed with PBS and flash frozen in liquid nitrogen.

Immunoprecipitation

The frozen cells were thawed in PBS and lysed in ice-cold lysis buffer (1% Triton X-100, 20 mM Tris-HCL (pH 7.4), 100 mM NaCl, 10% glycerol), containing 1 mM PMSF, 1 mM sodium orthovanadate and protease inhibitors: aprotinin, leupeptin and pepstatin (1μg/ml each). The lysis was achieved by incubation for 5 min on ice and by repetitive pippeting followed by passaging the cell suspension through a 10 ml syringe and 22G needle 10 times. Whole cell lysate (WCL) was than centrifuged at 21130 × *g* for 20 min at 4°C. WCL was pre-cleared from unspecific binders with 15 μl of PureProteome Protein A Magnetic Beads (Millipore). After incubation for 30 min at RT, the beads were discarded and the supernantant was used for immunoprecipitation (IP) of paxillin. For each of the samples 500 μl of supernatant obtained from 50 mg of wet cell pellet was incubated with increasing amount of sABs for 1 h at RT. sAB-paxillin complexes were then pulled-down by

incubating each sample with 50 µl PureProteome Protein A Magnetic Beads for 30 min at RT and analyzed by western blot.

For the competition IP experiments each of the LD-MBP fusions was pre-incubated with its corresponding sAB at 5 µM concentration for 1 h at RT. Then, 1.5 mM FAT domain was added and incubated for 1 h at RT. Protein complexes were then pulled down with 50 µl PureProteome Protein A Magnetic Beads after incubation for 30 min at RT. The amount of pulled down LD-MBP construct was detected by Western blot.

Western Blot

Beads containing immunoprecipitated proteins were mixed with 15 µl of 6× SDS Gel Loading Buffer, mixed and heated at 95°C for 10 minutes. The samples were then placed on the magnetic stand, allowing the beads to migrate to the magnet and the supernatant was loaded onto 15% SDS-PAG. After the electrophoresis the proteins were transferred to PVDF membrane (Thermo) for 30 min at 1 Amp and 25 V. Then the membrane was blocked in TBS containing 0.1% Tween 20 and 1% BSA at 4°C overnight. After blocking the membrane was incubated for 2 h at RT with primary IgG, washed and then incubated for 1 h at RT with HRP-conjugated secondary IgG. The following primary antibodies were used: anti-human paxillin (C-18) goat polyclonal antibody (Santa Cruz Biotechnology; 1:400), anti-human FAK (A-17) rabbit polyclonal antibody (Santa Cruz Biotechnology; 1:400), mouse anti 6xHis monoclonal antibody (Clontech; 1:500) for detection of MBP-LD His-tagged constructs after competition IP with recombinant purified FAT domain. Secondary antibodies: rabbit anti-goat IgG-HRP (Jackson ImmunoResearch; 1:2500), goat anti-rabbit IgG-HRP (Jackson ImmunoResearch; 1:2500), goat anti-mouse IgG-HRP (Jackson ImmunoResearch; 1:2500). Immun-Star WesternC Chemiluminescence Kit (BIO-RAD) was used for signal detection.

Preparation of fluorescently labeled sABs

For conjugation with maleimide-Cy5 fluorophore, a point mutation (A121C) in the heavy chain of the sAB was introduced. The purified mutant sABs were dialyzed into PBS pH 7.4 at 4°C overnight. To activate the introduced cysteine, 0.2 mg/ml of the sAB was incubated with 1 mM TCEP for 10 min at RT. Then maleimide-Cy5 fluorophore (GE Healthcare) in DMSO was added to the solution to a final concentration of 100 µM and the reaction was carried out for 2 h at RT with mild vortexing every 30 min. The labeled sABs were purified by gel filtration using a Econo-Pac 10DG desalting Column (GE Healthcare) equilibrated with PBS, pH 7.4 to remove excess of unbound fluorophore.

Immunofluorescence microscopy

A549 cells were grown in 12 well plates on 18 mm circular glass slides for 24 h. After reaching 1×10^5 density the cells were washed 3 times with PBS, fixed in 4% p-formaldehyde, permeablized in PBST pH 7.4, and blocked with 1% BSA in PBST for 30 min RT. Then slides were incubated with fluorescently labeled sAB for 1h at RT. For each 18mm glass slide 6 µg of Cy-5 labeled LD2 or LD4 sAB was used. Actin filaments were stained with Alexa Fluor 488-phalloidin (Invitrogen) for 30 min at room temperature. Nuclei were stained with Hoechst 33342 reagent (Invitrogen) for 5 min at room temperature, and

samples were mounted using ProLong Gold antifade reagent (Invitrogen). Single channel images were collected on Leica SP5 II STED-CW Super-resolution Laser Scanning Confocal microscope equipped with HCX PL APO CS 63.0× 1.40 OIL UV objective and on Zeiss AXIO Observer. A1 microscope equipped with ZEISS Plan-Apochromat 63x/1.40 Oil Ph3 objective. Multicolored image stacks were created from monochrome acquisitions using the Adobe Photoshop CS5 software.

Supplementary Material

Refer to Web version on PubMed Central for supplementary material.

Acknowledgments

This work was supported by National Institutes of Health grant no. U01 GM094588 and Chicago Biomedical Consortium. The authors would like to thank A. Koide, The University of Chicago, for kindly providing the phage library. This research used resources of the Advanced Photon Source (APS), a U.S. Department of Energy (DOE) Office of Science User Facility operated for the DOE Office of Science by Argonne National Laboratory under Contract No. DE-AC02-06CH11357. We gratefully acknowledge the support of The Northeastern Collaborative Access Team (NE-CAT) staff with data collection at the APS 24-ID-C beamline, which is funded by NE-CAT member institutions and the National Institute of General Medical Sciences (NIGMS). We would also like to thank the presenters of the 2012 CCP4/APS School for the advice and help with data processing (Nukri Sanishvili (APS) and Dominika Borek (UT Southwestern)) and molecular replacement (Ronan Keegan (STFC Rutherford Appleton Laboratory) and Gabor Bunkoczi (CIMR, University of Cambridge)) for LD2-sAB structure. Confocal microscopy imaging was performed at the University of Chicago Integrated Light Microscopy Facility with kind assistance of Dr. Christine Labno.

ABBREVIATIONS

FAK	focal adhesion kinase
ILK	integrin-linked kinase
LIM	LinII, Isl-1 and Mec-3 domain
FAT	focal adhesion targeting domain
Hic-5	hydrogen peroxide inducible clone
sABs	synthetic antibodies
CDRs	complementarity determining regions
MBP	maltose binding protein
SPR	surface plasmon resonance
ASU	asymmetric unit
RMSD	root-mean-square deviation
LIC	ligation independent cloning
PMPs	Paramagnetic Particles
RT	room temperature
cfu	colony-forming units
RU	response units

LDAO	n-Dodecyl-N, N-Dimethylamine-N-Oxide
WCL	whole cell lysate
IP	immunoprecipitation

References

1. Brown MC, Curtis MS, Turner CE. Paxillin LD motifs may define a new family of protein recognition domains. Nat Struct Biol. 1998; 5:677–8.10.1038/1370 [PubMed: 9699628]
2. Burridge K, Fath K, Kelly T, Nuckolls G, Turner C. Focal adhesions: transmembrane junctions between the extracellular matrix and the cytoskeleton. Annu Rev Cell Biol. 1988; 4:487–525.10.1146/annurev.cb.04.110188.002415 [PubMed: 3058164]
3. Clark EA, Brugge JS. Integrins and signal transduction pathways: the road taken. Science (80-). 1995; 268:233–9.
4. Craig SW, Johnson RP. Assembly of focal adhesions: progress, paradigms, and portents. Curr Opin Cell Biol. 1996; 8:74–85. [PubMed: 8791409]
5. Schwartz MA, Schaller MD, Ginsberg MH. Integrins: Emerging paradigms of signal transduction. Annu Rev Cell Dev Biol. 1995; 11:549–99.10.1146/annurev.cellbio.11.1.549 [PubMed: 8689569]
6. Turner CE, Glenney JR Jr, Burridge K. Paxillin: a new vinculin-binding protein present in focal adhesions. J Cell Biol. 1990; 111:1059–68. [PubMed: 2118142]
7. Brown MC, Turner CE. Paxillin: adapting to change. Physiol Rev. 2004; 84:1315–39.10.1152/physrev.00002.2004 [PubMed: 15383653]
8. Turner CE. Paxillin and focal adhesion signalling. Nat Cell Biol. 2000; 2:E231–6.10.1038/35046659 [PubMed: 11146675]
9. Sattler M, Pisick E, Morrison PT, Salgia R. Role of the cytoskeletal protein paxillin in oncogenesis. Crit Rev Oncog. 2000; 11:63–76. [PubMed: 10795627]
10. Salgia R, Li JL, Lo SH, Brunkhorst B, Kansas GS, Sobhany ES, et al. Molecular cloning of human paxillin, a focal adhesion protein phosphorylated by P210BCR/ABL. J Biol Chem. 1995; 270:5039–47. [PubMed: 7534286]
11. Turner CE, Miller JT. Primary sequence of paxillin contains putative SH2 and SH3 domain binding motifs and multiple LIM domains: identification of a vinculin and pp125Fak-binding region. J Cell Sci. 1994; 107(Pt 6):1583–91. [PubMed: 7525621]
12. Hildebrand JD, Schaller MD, Parsons JT. Paxillin, a tyrosine phosphorylated focal adhesion-associated protein binds to the carboxyl terminal domain of focal adhesion kinase. Mol Biol Cell. 1995; 6:637–47. [PubMed: 7579684]
13. Brown MC, Perrotta JA, Turner CE. Identification of LIM3 as the principal determinant of paxillin focal adhesion localization and characterization of a novel motif on paxillin directing vinculin and focal adhesion kinase binding. J Cell Biol. 1996; 135:1109–23.10.1083/jcb.135.4.1109 [PubMed: 8922390]
14. Nikolopoulos SN, Turner CE. Actopaxin, a new focal adhesion protein that binds paxillin LD motifs and actin and regulates cell adhesion. J Cell Biol. 2000; 151:1435–48. [PubMed: 11134073]
15. Nikolopoulos SN, Turner CE. Integrin-linked kinase (ILK) binding to paxillin LD1 motif regulates ILK localization to focal adhesions. J Biol Chem. 2001; 276:23499–505.10.1074/jbc.M102163200 [PubMed: 11304546]
16. Schaller MD. Paxillin: a focal adhesion-associated adaptor protein. Oncogene. 2001; 20:6459–72.10.1038/sj.onc.1204786 [PubMed: 11607845]
17. Tumbarello DA, Brown MC, Turner CE. The paxillin LD motifs. FEBS Lett. 2002; 513:114–8. [PubMed: 11911889]
18. Arold ST, Hoellerer MK, Noble MEM. The structural basis of localization and signaling by the focal adhesion targeting domain. Structure. 2002; 10:319–27.10.1016/S0969-2126(02)00717-7 [PubMed: 12005431]

19. Hayashi I, Vuori K, Liddington RC. The focal adhesion targeting (FAT) region of focal adhesion kinase is a four-helix bundle that binds paxillin. Nat Struct Biol. 2002; 9:101–6.10.1038/nsb755 [PubMed: 11799401]
20. Hoellerer MK, Noble ME, Labesse G, Campbell ID, Werner JM, Arold ST. Molecular recognition of paxillin LD motifs by the focal adhesion targeting domain. Structure. 2003; 11:1207–17. [PubMed: 14527389]
21. Liu G, Guibao CD, Zheng J. Structural insight into the mechanisms of targeting and signaling of focal adhesion kinase. Mol Cell Biol. 2002; 22:2751–60. [PubMed: 11909967]
22. Lorenz S, Vakonakis I, Lowe ED, Campbell ID, Noble ME, Hoellerer MK. Structural analysis of the interactions between paxillin LD motifs and alpha-parvin. Structure. 2008; 16:1521–31.10.1016/j.str.2008.08.007 [PubMed: 18940607]
23. Richardson A, Malik RK, Hildebrand JD, Parsons JT. Inhibition of cell spreading by expression of the C-terminal domain of focal adhesion kinase (FAK) is rescued by coexpression of Src or catalytically inactive FAK: a role for paxillin tyrosine phosphorylation. Mol Cell Biol. 1997; 17:6906–14. [PubMed: 9372922]
24. Stiegler AL, Draheim KM, Li X, Chayen NE, Calderwood DA, Boggon TJ. Structural basis for paxillin binding and focal adhesion targeting of beta-parvin. J Biol Chem. 2012; 287:32566–77.10.1074/jbc.M112.367342 [PubMed: 22869380]
25. Wang X, Fukuda K, Byeon IJ, Velyvis A, Wu C, Gronenborn A, et al. The structure of alpha-parvin CH2-paxillin LD1 complex reveals a novel modular recognition for focal adhesion assembly. J Biol Chem. 2008; 283:21113–9.10.1074/jbc.M801270200 [PubMed: 18508764]
26. Schaller MD, Parsons JT. pp125FAK-dependent tyrosine phosphorylation of paxillin creates a high-affinity binding site for Crk. Mol Cell Biol. 1995; 15:2635–45. [PubMed: 7537852]
27. Schaller MD. Biochemical signals and biological responses elicited by the focal adhesion kinase. Biochim Biophys Acta. 2001; 1540:1–21. [PubMed: 11476890]
28. Fellouse FA, Esaki K, Birtalan S, Raptis D, Cancasci VJ, Koide A, et al. High-throughput generation of synthetic antibodies from highly functional minimalist phage-displayed libraries. J Mol Biol. 2007; 373:924–40.10.1016/j.jmb.2007.08.005 [PubMed: 17825836]
29. Miller KR, Koide A, Leung B, Fitzsimmons J, Yoder B, Yuan H, et al. T cell receptor-like recognition of tumor in vivo by synthetic antibody fragment. PLoS One. 2012; 7:e43746.10.1371/journal.pone.0043746 [PubMed: 22916301]
30. Burridge K, Chrzanowska-Wodnicka M. Focal adhesions, contractility, and signaling. Annu Rev Cell Dev Biol. 1996; 12:463–518.10.1146/annurev.cellbio.12.1.463 [PubMed: 8970735]
31. Scheswohl DM, Harrell JR, Rajfur Z, Gao G, Campbell SL, Schaller MD. Multiple paxillin binding sites regulate FAK function. J Mol Signal. 2008; 3:1.10.1186/1750-2187-3-1 [PubMed: 18171471]
32. Feldhaus MJ, Siegel RW, Opresko LK, Coleman JR, Feldhaus JM, Yeung YA, et al. Flow-cytometric isolation of human antibodies from a nonimmune Saccharomyces cerevisiae surface display library. Nat Biotechnol. 2003; 21:163–70.10.1038/nbt785 [PubMed: 12536217]
33. Cobaugh CW, Almagro JC, Pogson M, Iverson B, Georgiou G. Synthetic antibody libraries focused towards peptide ligands. J Mol Biol. 2008; 378:622–33.10.1016/j.jmb.2008.02.037 [PubMed: 18384812]
34. Bertolucci CM, Guibao CD, Zheng J. Structural features of the focal adhesion kinase-paxillin complex give insight into the dynamics of focal adhesion assembly. Protein Sci. 2005; 14:644–52.10.1110/ps.041107205 [PubMed: 15689512]
35. Thomas JW, Cooley MA, Broome JM, Salgia R, Griffin JD, Lombardo CR, et al. The role of focal adhesion kinase binding in the regulation of tyrosine phosphorylation of paxillin. J Biol Chem. 1999; 274:36684–92. [PubMed: 10593973]
36. Otwinowski, Z.; Minor, W. [20] Processing of X-ray diffraction data collected in oscillation mode. In: Carter, Charles W., Jr, editor. Methods Enzym. Vol. 276. Academic Press; 1997. p. 307-26.http://dx.doi.org/10.1016/S0076-6879(97)76066-X
37. Kabsch W. Xds. Acta Crystallogr D Biol Crystallogr. 2010; 66:125–32.10.1107/S0907444909047337 [PubMed: 20124692]

38. McCoy AJ, Grosse-Kunstleve RW, Adams PD, Winn MD, Storoni LC, Read RJ. Phaser crystallographic software. J Appl Crystallogr. 2007; 40:658–74.10.1107/S0021889807021206 [PubMed: 19461840]

39. Winn MD, Ballard CC, Cowtan KD, Dodson EJ, Emsley P, Evans PR, et al. Overview of the CCP4 suite and current developments. Acta Crystallogr D Biol Crystallogr. 2011; 67:235–42.10.1107/S0907444910045749 [PubMed: 21460441]

40. Murshudov GN, Skubak P, Lebedev AA, Pannu NS, Steiner RA, Nicholls RA, et al. REFMAC5 for the refinement of macromolecular crystal structures. Acta Crystallogr D Biol Crystallogr. 2011; 67:355–67.10.1107/S0907444911001314 [PubMed: 21460454]

41. Emsley P, Lohkamp B, Scott WG, Cowtan K. Features and development of Coot. Acta Crystallogr D Biol Crystallogr. 2010; 66:486–501.10.1107/S0907444910007493 [PubMed: 20383002]

42. Schrodinger LLC. The PyMOL Molecular Graphics System, Version 1.3r1. 2010.

Highlights

- Inhibition of paxillin-mediated signaling can be achieved by blocking LD motifs
- High-affinity, specific antibodies for LD2 and LD4 were generated by phage display
- Crystal structures show that the antibodies bind native helical state of LD motifs
- The antibodies recognize paxillin in cells and inhibit LD-FAT interaction in vitro
- Generated inhibitory antibodies are tools for investigation of paxillin signaling

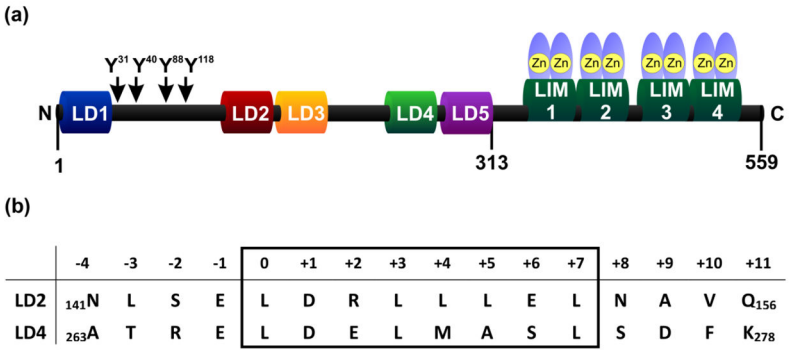

Fig. 1. Paxillin structure and LD motifs

(a) Modular structure of paxillin. The scheme includes five LD motifs and four LIM domains. LD2 and LD4 serve as interfaces binding FAT domain of FAK. Also shown are four Y residues that can be phosphorylated. The scheme is not drawn to scale. **(b)** Sequences of LD2 and LD4 motifs used in selection experiments. The peptides used during selection contained core 8 amino acids (the box) plus additional 4 amino acids flanking the core on N- and C-termini, that are believed to augment the specificity of binding of paxillin to the partners.

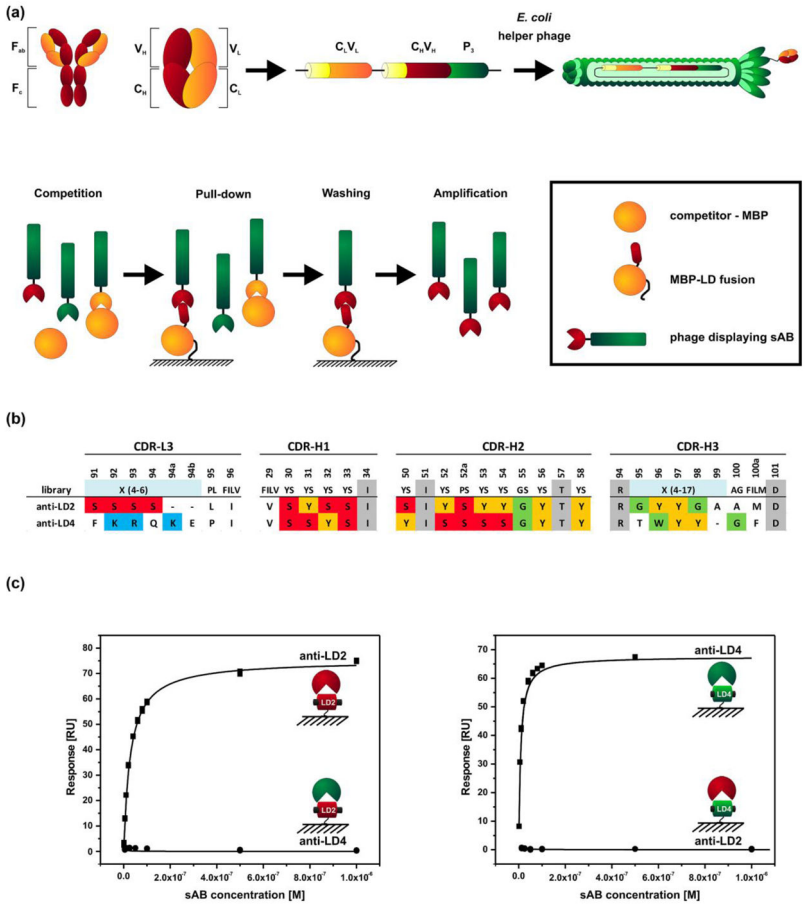

Fig. 2. Phage selection against LD2 and LD4 peptides

(a) Fab fragments cloned into phagemid bearing a sequence coding for phage pIII surface protein were displayed on phage surface after infection of *E. coli* cells with M13-KO7 helper phage. The LD motifs fused to MBP were used during selection. The phage library was first incubated with isolated MBP to get rid of MBP binders. Next, biotinylated fusion protein was added. After binding, the fusion was pulled down with magnetic beads and washed. The pulled down phage was then amplified and used for the next round of selection. Four rounds of panning were performed against LD2 and LD4 fused to MBP. **(b)** Sequences of four randomized Complementarity Determining Regions (CDRs) (L1, H1, H2 and H3) of two clones that were selected during biopanning against LD2 and LD4. Above the sequences are shown residues that were allowed at particular position in the phage library. Where no particular residue is shown, any amino acid was possible. Color coding: grey - residues not randomized; red – S; yellow – Y; green – G. **(c)** Equilibrium SPR data for LD-sAB binding. Either LD2-MBP or LD4-MBP fusion was captured *via* His-tag on nickel chip and binding of each of the sABs was analyzed. Dissociation constant of LD2-sAB complex was estimated to be ~24 nM and dissociation constant of LD4-sAB complex was assessed to be ~6 nM. The sABs are entirely orthogonal, as no binding between LD motifs and non-corresponding sABs was detected.

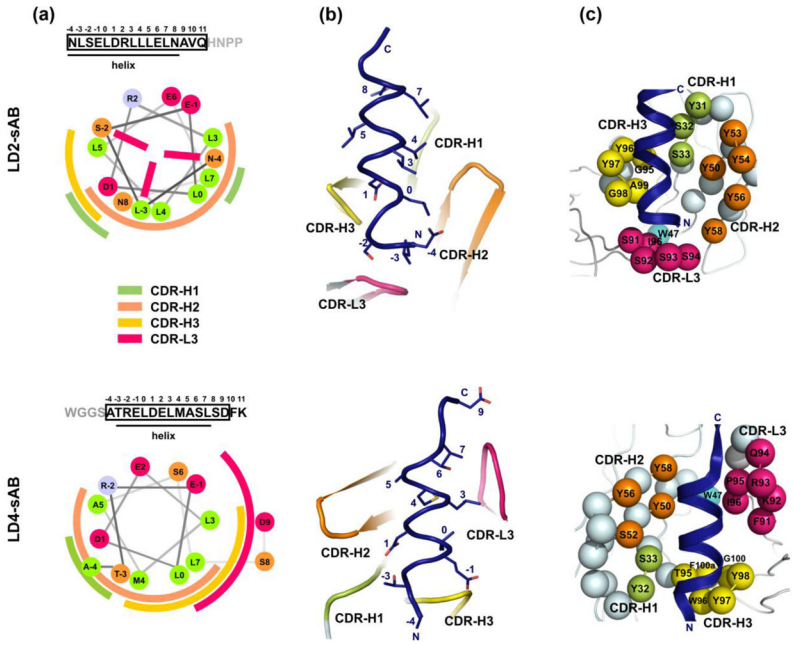

Fig. 3. LD-sAB crystal structures

(a) Sequences of peptides used for crystallization and their helical wheel representation based on sAB-LD structures. Sequences in black – sequences of peptides used during biopanning; grey – additional fragments in peptides used in crystallization that were not part of the peptides during selection. Parts of peptides with visible electron density in sAB-LD structures are in boxes. Lines under the sequences indicate the parts of the peptides found to adopt helical conformation in the LD-sAB structures. The helical wheel representations show amino acids that interact with individual CDRs of sABs – shown as arcs of different colors. Color coding for CDRs: green - H1; orange - H2; yellow - H3; pink - L3. Color coding in the helical wheel representation of the peptides: green - hydrophobic residues; orange - neutral residues; red - acidic residues; blue - basic residues. **(b)** Top view of the peptides (dark blue) within the sAB binding pockets formed by CDR H1, H2, H3 and L3. The shown side chains correspond to the LD peptide residues that take part in sAB binding. **(c)** sAB residues taking part in peptide binding. The residues from diversified CDRs are shown as spheres. The residues taking part in peptide binding are colored and numbered.

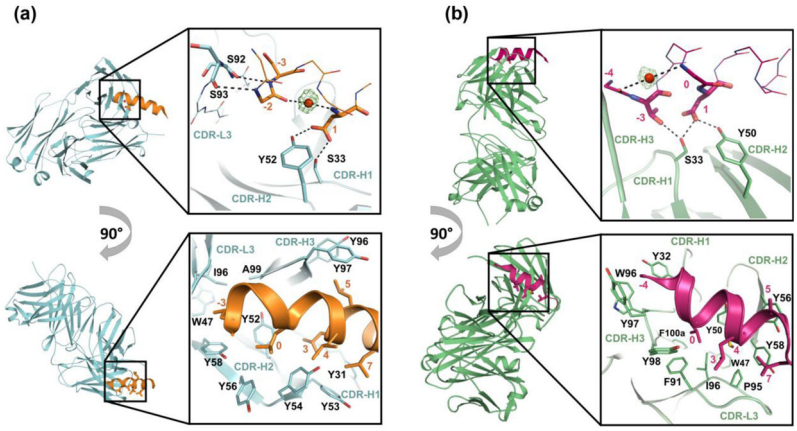

Fig. 4. LD-sAB interactions

(a) and (b) Interactions between sABs and LD2 and LD4, respectively. Hydrogen bonds (top panels) and hydrophobic interactions (bottom panels) formed at the LD-sAB interfaces. LD2 and its corresponding sAB are shown in orange and cyan, respectively. LD4 and its corresponding sAB are shown in pink and green, respectively. In top panels hydrogen bonds are shown as dashed lines and interacting residues are shown as thick sticks. Water molecules are depicted as red spheres surrounded by omit difference F_O-F_C maps contoured at 3.0 σ. The maps were obtained by simulated annealing.

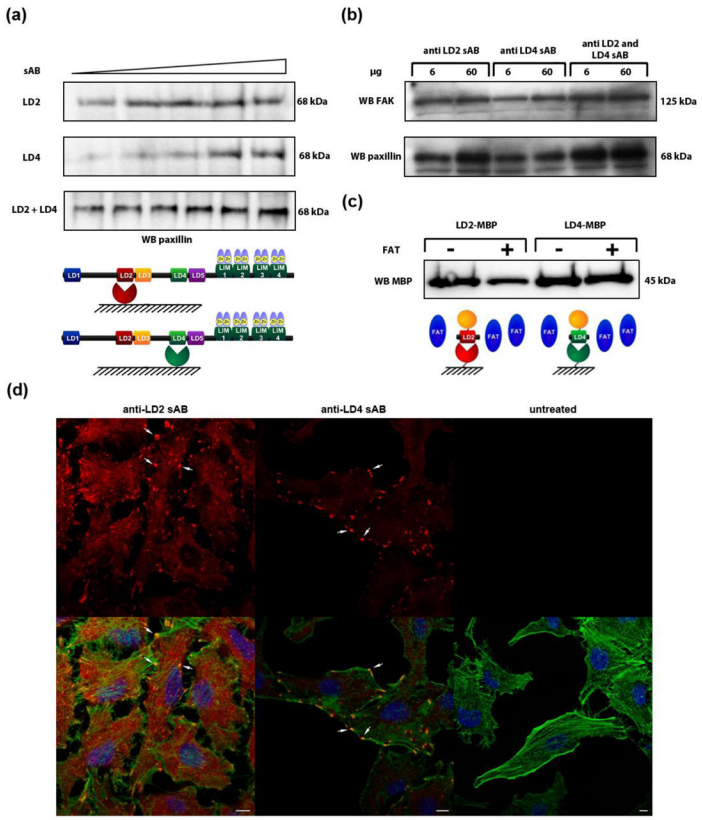

Fig. 5.

(a) Top panel: immunoprecipitation of endogenous paxillin from cell lysates using LD2 and LD4 sABs. Native paxillin from lung cancer A549 cell line lysates was immunoprecipitated with increasing amounts of anti LD2 sAB and anti LD4 sABs resulting in detection of increasing amounts of paxillin of proper 68 kDa mass by anti-human paxillin IgG on Western Blot. Bottom panel: schematic representation of sABs bound to native paxillin molecule. **(b)** Paxillin was immunoprecipiatated from A549 lung cancer cell lysate with LD2 and LD4 sABs and the pulled down complexes were visualized either by anti-paxillin or anti-FAK antibody. **(c)** Competition IP. Competition of FAT domain of FAK with a complex of anti LD2 sAB and LD2-MBP or anti LD4 sAB and LD4-MBP. 1.5mM FAT is incubated with 5µM of each of the sAB and a corresponding LD-MBP construct. Top panel: Western Blot of immunoprecipitated complexes of anti LD motif sAB and corresponding LD-MBP construct. Bottom panel: schematic representation of FAT domain competition with anti LD sAB for binding the LD-MBP construct. **(d)** Immunostaining of native paxillin in A549 cells with Cy-5 labeled LD2 and LD4 sABs. A549 cells were stained with Cy-5 labeled LD2 and LD4 sAB (red) or were left untreated as a control. Arrowheads point to sites where sABs are bound to paxillin present in focal adhesions. Nuclei were counterstained with Hoehst (blue) and actin filaments were stained with Alexa-488 phalloidin (green). Scale bar corresponds to 10µm. Top panel: isolated red channel representing fluorescence signal from Cy-5 labeled sAB only. Bottom panel: three merged channels representing fluorescence signals from nuclear, actin and paxillin staining.

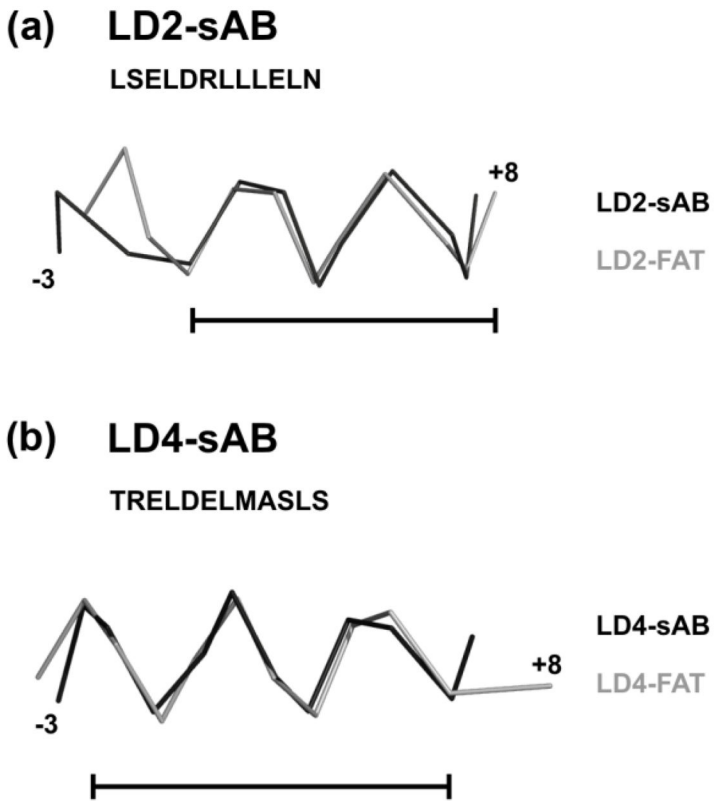

Fig. 6. Comparison of LD conformation in structures with sABs and FAT

(a) and (b) Superposition of LD helices from sAB-LD (dark grey) and FAT-LD (light grey) structures. The ribbons encompass 12 amino acid fragments, LSELDRLLLELN of LD2 and TRELDELMASLS of LD4. The RMSD between 10 Cα atoms (the lines) of the two superposed helices are 0.517 Å for LD2 and 0.602 Å for LD4. LD2-FAT structure; PDB: 1OW8. LD4-FAT structure; PDB: 1OW7.

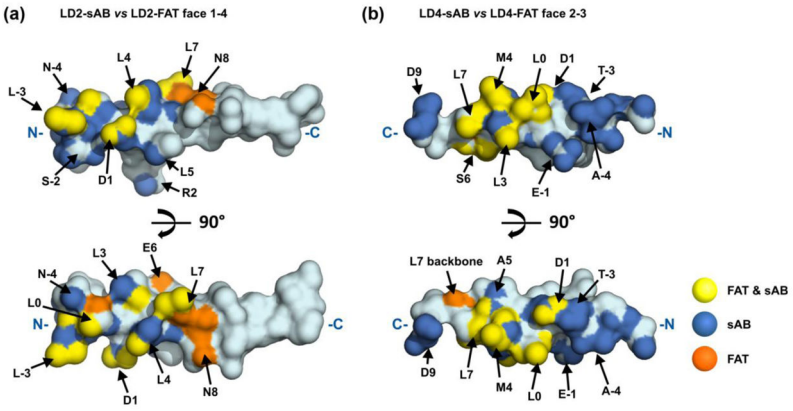

Fig. 7. Comparison of LD-sAB and LD-FAT interactions

Peptides from LD-sAB structures are shown as surface representation. The peptide atoms that are within 4 Å from either the sAB or FAT domain are colored; yellow – atoms shared by sABs and FAT; blue – atoms interacting with sABs only; orange - atoms interacting with FAT only. **(a)** Atoms contacting FAT have been selected based on LD2 interactions with the first binding site on FAT (face 1–4; PDB: 1OW8). **(b)** Atoms contacting FAT have been selected based on LD4 interactions with the second binding site on FAT (face 2–3; PDB: 1OW7).

Table 1

Data collection and refinement statistics

	LD2 sAB	LD4 sAB
Data collection		
Beam line/X-ray source	APS 24-ID-C	APS 24-ID-C
Wavelength (Å)	0.9792	0.9792
Space group	P1	$P2_12_12_1$
Cell dimensions		
a, *b*, *c* (Å)	108.19, 111.00, 143.86	117.41, 137.69, 223.57
α, *β*, *γ* (°)	94.65, 95.28, 114.53	90.00, 90.00, 90.00
Resolution (Å)	142.00-2.50 (2.50–2.64)[a]	117.50-2.00 (2.20-2.00)[a]
No. of observed/unique reflections	477864/207767	1117494/228060
R_{merge}	0.091 (0.721)[a]	0.155 (0.997)[a]
I/σ(I)	7.4 (1.1)[a]	7.6 (1.76)[a]
Completeness (%)	94.3 (94.2)[a]	93.2 (84.2)[a]
Redundancy	2.3 (2.3)[a]	4.9 (3.8)[a]
Refinement		
Resolution (Å)	142.0-2.50	117.50-2.00
No. reflections	185949	216648
R_{work}/R_{free}	0.2275/0.2447	0.226/0.2580
No. atoms	40426	21723
Protein	39989	20011
Water	377	1556
Other	60	156
B-factors (Å^2)		
Total	50.8	27.3
Protein	51.0	31.6
Water	32.7	34.3
Other	42.4	46.6
R.m.s.d.		
Bond lengths (Å)	0.0060	0.0060
Bond angles (°)	1.0730	1.1690
Ramachandran plot		
Most favored (%) or Favored	96.1	95.5
Allowed (%)	3.6	4.2
Disallowed (%) or outlier	0.3	0.3
PDB ID	4XGZ	4XH2

[a] Values in parenthesses refer to the data in the highest resolution shell.